

ORIGINAL ARTICLE

S.A. Zoubi · M.D. Williams · T.M. Mayhew
R.A. Sparrow

Number and ultrastructure of epithelial cells in crypts and villi along the streptozotocin-diabetic small intestine: a quantitative study on the effects of insulin and aldose reductase inhibition

Received: 18 April 1995 / Accepted: 26 June 1995

Abstract This study has quantified the effects of insulin treatment with and without aldose reductase inhibitor (ponalrestat) on intestinal epithelial cell morphology in streptozotocin-diabetic rats. Epithelial volumes, villous and microvillous surface areas and mean volumes of cells (and their nuclei) in crypts and villi were estimated in each of four segments and in the entire intestine. We derived total numbers of cells, quantified the ultrastructural features of average cells and explored variation along the intestine and between experimental groups. In crypts, insulin and ponalrestat had significant effects on cell number (reduced towards normal values) and size (volume and apex area increased beyond normal values). There were interaction effects between insulin and ponalrestat for cell volume and apex area (insulin producing more exaggerated effects when given without ponalrestat). On villi, insulin and ponalrestat returned cell numbers towards normal values but neither treatment normalised cell size or the number and area of microvilli per cell. Indeed, ponalrestat increased microvillous number and area beyond values found in untreated diabetic animals. Again, there were interaction effects between insulin and ponalrestat. Patterns of segmental variation seen in crypts of normal rats (values tending to be higher in proximal or mid-intestinal regions) were not preserved, and only some of the segmental differences seen on villi (higher values at proximal or mid-intestinal sites) were maintained during therapy. Apart from reducing the abnormally high numbers of cells in untreated diabetic rats, these results show that insulin and ponalrestat treatment fail to reconstitute epithelial cell morphology in the small intestines of experimental diabetic rats.

Key words Diabetes · Insulin · Aldose reductase inhibition · Small intestine · Epithelial cells

Introduction

There is experimental evidence that the small intestine responds to experimental diabetes with hyperplasia and hypertrophy [10, 23–25, 27, 29, 33, 40, 42, 43, 45, 51, 53, 54]. Small intestines of experimental-diabetic rats are heavier than normal, with taller villi and longer crypts. DNA content and protein/DNA ratio are elevated and there is greater crypt activity and a reduction in epithelial turnover times. Near the tips of villi in jejunal segments, epithelial cells are taller and tissue sections through villi contain more cell profiles. The marginal and central vessels of intestinal villi alter in calibre diameter and display decreased numbers and diameters of endothelial fenestrations. Increases occur in capillary pressure, capillary filtration rate and intestinal transport activities. These changes may not affect all parts of the intestine equally. Whilst there is little information concerning differential effects along the crypt-villus axis, evidence exists for such effects along the intestinal long axis. Structural, biochemical, physiological and kinetic studies indicate a greater impact in distal regions [33, 40, 46, 53, 54].

In light microscopic (LM) studies on streptozotocin-diabetic (STZ-diabetic) rats, we have confirmed that they have wider small intestines than age-matched controls, with greater volumes and surface areas of villi and crypts. Alterations in the heights and shapes of villi and the sizes of crypts were also observed [33]. At the ultrastructural level, STZ-diabetes did not alter the mean length, diameter or packing density of microvilli on villous epithelial cells suggesting that an increase in cell number is the principal adaptive response [30, 55]. A preferential effect in distal segments of small intestine was also indicated [30, 33].

Recently, we showed that STZ-diabetes leads to proliferative and hypertrophic responses within crypts but that the changes on villi are essentially hyperplastic [60]. Crypt cells became fatter but not taller, and the increase in their number was accompanied by an equivalent increase, about 80%, in the number of villous epithelial cells. However, villous cells were normal in size (nuclear

volume, cell height, area and volume) and in the number and surface area of their microvilli. Significant differences between segments were confined to the numbers and sizes of crypt cells and their nuclei.

The present study explores the effects on STZ-diabetic intestines of alternative forms of therapeutic intervention, viz conventional insulin injection and administration of an aldose reductase inhibitor, ponalrestat (ICI, Macclesfield, UK). In previous LM studies, we found that ponalrestat had no beneficial effects: small intestines were responsive to insulin (which restituted normal volumes and surface areas of villi and crypts) and the insulin response varied with intestinal region [36]. Here, effects are examined further by quantifying the fine structure of crypt and villous epithelial cells [55, 59, 60]. Since intestinal epithelium is a continuously renewing epithelium, the average cell data were supported by estimates of total cell numbers in the entire organ [37, 59, 60].

Materials and methods

Animals

As part of a larger study [6, 33, 36, 55, 59, 60], a total of 60 male Sprague-Dawley rats (11 weeks old, 350–550 g body weight) were divided into six groups of equal size and roughly equal mean body weight. They were housed in plastic cages on a 14 h–10 h light–dark cycle, fed a standard pellet diet and allowed *ad libitum* access to drinking water.

In an onset control group, animals were killed at 11 weeks. All other groups were maintained until 23 weeks of age before being weighed and killed under anaesthesia. One of these groups comprised age-matched control rats and the others were STZ-diabetic rats. To induce diabetes at 11 weeks, buffered STZ was injected *i.p.* (median dosage: 58 mg/kg body weight) under ether anaesthesia. Blood glucose levels rose to above 14 mmol/l within 2 days of injection. STZ-diabetic rats were divided into four groups: untreated diabetic rats (UD) and diabetic rats treated with daily *s.c.* injections of Ultralente insulin (ITD), ponalrestat alone (PTD) and insulin+ponalrestat (ITPTD). Ponalrestat (25 mg/kg) was administered daily by gavage. For this study, $n=6$ rats were randomly selected (by lottery) from each of the STZ-diabetic groups.

At 23 weeks of age, animals were killed at the same time of day by intracardiac perfusion with an isotonic saline pre-wash followed by 2.5% glutaraldehyde in Millonig's phosphate buffer at room temperature (pH 7.3). Perfused intestines were cut at pyloric and ileocolic junctions, freed of attached mesentery and removed entire.

Tissue sampling and microscopy

Full details of tissue sampling, including diagrams, are given elsewhere [30, 38]. Each intestine was cut transversely into four segments of roughly equal length. Segments were sliced into shorter pieces, one of which was chosen at random. After flushing out the lumen with fixative, each piece was trimmed and washed in buffer. Pieces were fixed secondarily for 2 h in 1% phosphate-buffered osmium tetroxide, dehydrated in graded ethanols and embedded in resin in flat moulds. They were subsequently glued to dummy blocks at standard orientation.

Complete transverse sections (0.5–1.0 μm thick) were stained with toluidine blue and viewed as projected images at final enlargements of $\times 39$ –72 (low power) and $\times 109$ (high power) calibrated with micrometer scale standards. Low-power sections were

viewed entire, but systematic random samples [20] of high-power fields were selected with the aid of the x,y scales on the LM stage.

For transmission electron microscopy (TEM), the same blocks were trimmed [35] and ultrathin sections (ca. 60 nm thick) were cut. These were contrasted with lead citrate and uranyl acetate, mounted on copper support grids and examined by TEM at 80 kV. Epithelia (crypts, villi) were sampled uniformly at low power using local vertical windows [5], i.e. full-thickness slices orthogonal to the epithelial surface. Sets of 3–4 fields per section were recorded and photomontages printed at $\times 5240$ using carbon grating replicas as external calibration standards. Further sets of 5–10 random fields showing the villous surface were sampled and printed at $\times 22600$.

Stereological analyses

As used here, the term “villous” includes non-cryptal intervillous mucosa as well as the epithelium that invests the villi themselves [59]. Villous and crypt volumes per segment were obtained from low-power LM fields by multiplying estimated cross-sectional areas by segment length [31, 32, 34]. Villous surface areas were estimated by intersection counting [30, 34]. Epithelial volumes per segment were estimated from point counts made on high-power LM projections.

Volume densities of nuclei within epithelium were determined on TEM fields from point counts and volume-weighted mean nuclear volumes from point-sampled intercept length measurements [19]. Analyses were performed using test lattices bearing points and parallel straight lines superimposed on fields at sine-weighted angles [5, 11, 19]. The product of nuclear volume density and epithelial volume provided total nuclear volume in each segment. Dividing this by mean nuclear volume gave the number of epithelial nuclei in each segment [59]. Numbers of crypt and villous cells (whether columnar absorptive epithelial, enteroendocrine, goblet or Paneth cells, etc) were estimated separately. Cell numbers are biased (i.e. slightly underestimated) because the volume-weighted mean volume of nuclei is somewhat greater than the number-weighted mean volume. The actual error is determined by the volume–frequency distribution of nuclei [11, 19], but epithelial cell nuclei are rather uniform in size and the bias is not important [13, 38] for the comparisons drawn here.

Relative and absolute surface areas and numbers of microvilli on villous cells were estimated by intersection and profile counting [30, 55]. Diameters and lengths of appropriately sectioned microvilli were used to calculate packing densities at the cell apex. Data were corrected for overprojection effects [18].

Mean cell height was calculated by dividing epithelial volume by surface area. Dividing estimates of villous surface by cell number gave a mean area equivalent to that of the microvillus-free cell apex (or of the cell base, i.e. the area of attachment to underlying basal lamina). Note that the product of this area and cell height is cell volume. From estimated cell numbers and total microvillous surfaces and numbers, the surface area and number of microvilli per average villous epithelial cell were derived. We did not collect these data for crypt cells.

Statistics

Segmental values were expressed as group means and standard errors of means (SEMs) before summing to obtain values for the entire small intestine. Trends in the apparent differences between segments were tested using Page's 'L' trends test ($k=4$ segments, $n=6$ rats), which is appropriate for related samples [41]. Differences between groups were examined using two-way analyses of variance [52] with insulin and ponalrestat as the two main effects. This test generates an interaction term that indicates the extent to which the effects of one factor (e.g. insulin treatment) are influenced by the effects of another (e.g. ponalrestat treatment). In the present context, interactions may involve synergistic or antagonistic effects between insulin and ponalrestat. The null hypothesis (no

difference between samples) was rejected if the *P* value was less than 0.05 for the specified degrees of freedom (*df*=1,20 for main and interaction effects).

Results

For information, age-matched control rats contained $3.32 (0.32) \times 10^9$ crypt epithelial cells of mean height 20 (0.5) μm , nuclear volume 56 (2.90) μm^3 , cell volume 207 (17.5) μm^3 and apex area 10.3 (0.98) μm^2 . Where segmental differences existed, values tended to be greater in proximal or mid-intestinal segments. All variables, except cell height, were greater in UD rats which also displayed far fewer segmental differences. In addition, con-

trols contained $5.10 (0.62) \times 10^9$ villous epithelial cells. However, the dimensions and microvillous characteristics of villous cells were not significantly different from those in UD animals. STZ-diabetes affected the numbers of crypt and villous cells equally (both were about 80% higher than in age-matched control rats), so that the ratio of villous:crypt cells was unaltered.

Effects of treatments

The structural quantities in the entire small intestine, and the main and interaction effects of insulin and ponalrestat, are summarised in Tables 1–3 and Fig. 1.

Fig. 1 Three-dimensional summary of the morphological variations (cell height, apex area, volume and nuclear content) due to diabetes and treatment with insulin and/or ponalrestat. Each column represents the average epithelial cell in the crypts or villi of a given group (UD untreated diabetics, ITD insulin-treated diabetics, PTD ponalrestat-treated diabetics, ITPTD insulin+ponalrestat-treated diabetics; AMC age-matched controls, given for reference). Cell heights and apex areas are to scale and nuclear volume is indicated by stippling at the base of each column. Groups are arranged vertically, and solid lines running between columns indicate differences (if any) in cell height and width from those in AMC rats. Running from left to right is the crypt-villus axis, and broken lines indicate differences (if any) in cell height and width between crypts and villi within a group. For further details, see text and Tables 1–3

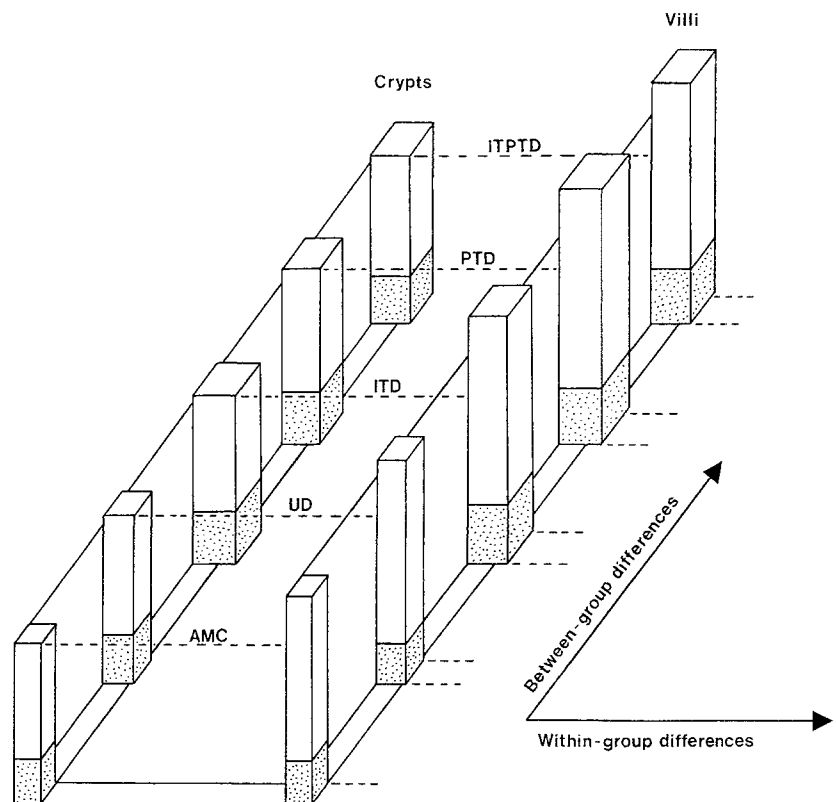


Table 1 Cell number and morphophenotype in crypt epithelium of treated and untreated STZ-diabetic rats. Values are group means with SEM in round brackets (UD untreated diabetic rats, ITD, diabetic rats treated daily with Ultralente insulin s.c., PTD diabetic rats treated with ponalrestat alone, ITPTD diabetic rats treated with insulin+ponalrestat)

Variable	Experimental-diabetic groups			
	UD	ITD	PTD	ITPTD
Cell number ($\times 10^9$)	5.91 (0.77)	2.14 (0.28)	3.65 (0.39)	1.61 (0.11)
Cell height (μm)	21 (0.54)	21 (0.50)	22 (0.42)	21 (0.48)
Nuclear volume (μm^3)	82 (10.0)	188 (14.4)	162 (13.6)	170 (18.0)
Cell volume (μm^3)	304 (37.9)	613 (51.2)	543 (34.7)	609 (42.7)
Cell surface without microvilli (μm^2)	14.8 (1.60)	30.2 (3.09)	24.7 (1.73)	29.7 (1.56)

Table 2 Cell number and morphophenotype in villous epithelium of treated and untreated STZ-diabetic rats. Values are group means (SEM)

Variable	Experimental-diabetic groups			
	UD	ITD	PTD	ITPTD
Cell number (x 10 ⁹)	9.14 (1.53)	2.43 (0.16)	4.64 (0.53)	2.31 (0.18)
Cell height (μm)	28 (1.29)	31 (1.39)	32 (1.20)	30 (0.84)
Nuclear volume (μm ³)	74 (5.18)	203 (9.04)	197 (11.7)	189 (16.9)
Cell volume (μm ³)	444 (45.8)	839 (40.7)	914 (75.8)	812 (59.3)
Cell surface without microvilli (μm ²)	16.0 (1.83)	27.8 (1.81)	29.2 (2.60)	27.1 (2.81)
Cell surface with microvilli (μm ²)	214 (25.1)	426 (22.4)	414 (35.5)	394 (39.8)
Number of microvilli per cell	560 (66.0)	891 (57.9)	1104 (103)	947 (97.0)
Villus : crypt cell number ratio	1.81 (0.52)	1.21 (0.13)	1.33 (0.20)	1.45 (0.12)

Table 3 Results of two-way analyses of variance applied to structural quantities in treated and untreated STZ-diabetic rats (see Tables 1 and 2)

Variable	Main and interaction effects		
	Insulin	Ponalrestat	Interaction
Cell number (x10 ⁹)			
Crypts	<i>P</i> <0.001	<i>P</i> <0.01	NS
Villi	<i>P</i> <0.001	<i>P</i> <0.01	<i>P</i> <0.05
Cell height (μm)			
Crypts	NS	NS	NS
Villi	NS	NS	NS
Nuclear volume (μm ³)			
Crypts	<i>P</i> <0.001	<i>P</i> <0.05	<i>P</i> <0.01
Villi	<i>P</i> <0.001	<i>P</i> <0.001	<i>P</i> <0.001
Cell volume, (μm ³)			
Crypts	<i>P</i> <0.001	<i>P</i> <0.05	<i>P</i> <0.01
Villi	<i>P</i> <0.05	<i>P</i> <0.001	<i>P</i> <0.001
Cell surface without microvilli (μm ²)			
Crypts	<i>P</i> <0.001	<i>P</i> <0.05	<i>P</i> <0.05
Villi	<i>P</i> <0.05	<i>P</i> <0.05	<i>P</i> <0.01
Cell surface with microvilli, (μm ²)			
Villi	<i>P</i> <0.01	<i>P</i> <0.05	<i>P</i> <0.01
Number of microvilli per cell			
Villi	NS	<i>P</i> <0.01	<i>P</i> <0.01

In crypts, insulin injection had significant effects on all variables except cell height (Tables 1, 3). Insulin returned cell numbers towards normal levels but led to further increases in cell size (nuclear volume, cell volume and cell apex area) beyond those due to induced diabetes. Ponalrestat also tended to normalise cell numbers and increase cell sizes further (see Fig. 1). There were significant interaction effects between treatments for cell volumes and apex areas (Table 3), with insulin tending to have greater effects when given without ponalrestat.

On villi, insulin had significant effects on all variables except cell height and number of microvilli per cell (Tables 2, 3). Cell numbers were reduced to below those found in UD rats but also fell below values found in age-matched controls. In contrast, volumes and apex areas were greater than in UD rats and, by implication, greater than normal (Fig. 1). The surface area and number of microvilli per cell were also greater than in UD rats. Ponalrestat had significant effects on all variables except cell height. Again, cell numbers, but not cell dimensions, returned towards normal values (Fig. 1). There were statistically significant insulin×ponalrestat interaction effects on all quantities except cell height. In each case, insulin treatment produced greater effects when given without ponalrestat treatment.

The numerical ratio of villus:crypt cells was not altered by insulin or ponalrestat treatments (since these did not change during diabetes), and there was no interaction effect between treatments.

Segmental differences

These are summarised in Table 4. For comparison, crypt cell size and number in age-matched control rats tended to be higher in proximal or mid-intestinal segments. Villous cells showed segmental trends for all variables except the surfaces and numbers of microvilli per average cell. STZ-diabetes abolished some of the segmental differences, but not those related to crypt cell volumes or the number of villous epithelial cells.

Insulin did not reconstitute normal segmental trends seen in crypts and crypt cells but did normalise some of those in villi. Similar results were found with ponalrestat, which also restored normal trends in crypt cell volumes. The combined use of insulin and ponalrestat returned fewer segmental trends to normal patterns.

Table 4 Results of Page's L trends test applied to segmental estimates of structural quantities in treated and untreated STZ-diabetic rats

Variable	Experimental-diabetic groups			
	UD	ITD	PTD	ITPTD
Cell number ($\times 10^9$)				
Crypts	NS	NS	NS	NS
Villi	$P < 0.05$	$P < 0.05$	$P < 0.05$	$P < 0.05$
Cell height (μm)				
Crypts	NS	NS	NS	$P < 0.01$
Villi	NS	$P < 0.01$	NS	$P < 0.01$
Nuclear volume (μm^3)				
Crypts	$P < 0.05$	NS	$P < 0.05$	NS
Villi	NS	$P < 0.01$	$P < 0.05$	NS
Cell volume (μm^3)				
Crypts	NS	NS	$P < 0.05$	$P < 0.01$
Villi	NS	$P < 0.01$	$P < 0.01$	NS
Cell surface without microvilli (μm^2)				
Crypts	NS	NS	NS	NS
Villi	NS	$P < 0.05$	$P < 0.01$	NS
Cell surface with microvilli (μm^2)				
Villi	NS	$P < 0.01$	$P < 0.01$	$P < 0.05$
Number of microvilli per cell				
Villi	$P < 0.05$	$P < 0.01$	$P < 0.01$	NS

Vertical differences

As cells moved along the crypt-villus axis they became more voluminous, and this could be attributed to changes in cell height rather than girth (Tables 1, 2, Fig. 1).

Discussion

This study has quantified epithelial cell number and ultrastructure in crypts and villi of small intestines from untreated, insulin-treated, ponalrestat-treated and insulin+ponalrestat-treated diabetic rats. In previous studies [60], we have shown that the adaptive response of crypts in 12-week STZ-diabetic rats is hyperplastic and hypertrophic. Crypt cell number almost doubled and mean cell volume rose by about 50%. In contrast, the villous response involved solely net cell recruitment, the villus:crypt cell ratio being maintained and villi bearing 80% more cells of essentially normal morphology. In passing from crypt to villus, the average cell became taller and more voluminous but, at least in STZ-diabetic animals, not fatter.

Effects of treatments

Insulin and ponalrestat tend to reduce cell numbers (though not necessarily to normal values), but fail to maintain or restore normal cell phenotype. This is surprising given previous findings that insulin therapy normalises intestinal absorption, blood glucose levels, and enzyme activities [10, 22, 46, 57] as well as villous surface area and the volumes of villi and crypts [33, 36]. It appears that the morphological changes that normalise

the volumes and absorptive surfaces of villi and volumes of crypts are due to the presence of fewer but larger epithelial cells. Ponalrestat failed to normalise villous surface areas or crypt and villous volumes [36]. Indeed, crypt volumes were greater than in UD rats. In this sense at least, the effects of ponalrestat on the crypts are less beneficial than those of insulin.

Studies on villous epithelial cells in STZ-diabetic rats have demonstrated that insulin affects the extent to which microvilli amplify the apical cell surface via changes in their length, diameter and packing density [55]. Ponalrestat influenced amplification mainly by altering packing densities. Present results indicate that these changes are accompanied by increases in the number and surface of microvilli per average cell in insulin- and ponalrestat-treated animals and that these, in turn, are determined by the increases in cell apex area. This explains why the effects of insulin therapy normalise villous surface area and microvillous surface area in the whole organ [33, 36, 55].

The insulin effects are intriguing. At the cellular level, its effects on crypts and villi are not markedly different from those of ponalrestat, save for a more exaggerated depletion of cell number. Depletion of endogenous insulin via administration of STZ appears to result in cellular changes which are not restored by injection of exogenous insulin and which vary somewhat between crypts and villi. Depletion leads to increased cell numbers in crypts and on villi, but also to crypt cell hypertrophy without consequent changes in the volumes of villous cells. Injecting exogenous insulin does not normalise cell size. On the contrary, it leads to further cell hypertrophy. Moreover, whilst it tends to normalise crypt cell number, it produces below-normal complements of villous cells.

The exact role of insulin in the regulation of cell proliferation is unclear. It is known to influence intestinal absorption of polyamines (which are important in intestinal maturation and cell proliferation during weaning) and to stimulate the rate-limiting enzyme of polyamine synthesis (ornithine decarboxylase) in mature cells [9]. Inhibitors of this enzyme prevent hyperplasia in STZ-diabetic rats [58]. However, recent evidence suggests that whilst insulin affects the expression of intestinal enzymes, it does not have a major role in regulating cell proliferation [9, 17]. The latter could be mediated by insulin-like growth factors (IGFs), which share a number of actions and amino acid sequences with insulin and exhibit high levels of expression on crypt cells [14, 16, 21, 26, 47]. However, other growth factors may be involved [2].

Segmental differences

Although not detailed here, significant segmental trends were detected in all groups of rats. Our findings for age-matched controls [59] are consistent with longitudinal gradients of villous morphology and activity described by others in normal animals. Proximal segments are more important in nutrient digestion and transport and tend to have more cells, greater absorptive surface areas and higher villus: crypt cell ratios [4, 24, 30, 34, 56, 59].

Various studies have shown that experimental diabetes disturbs normal patterns of segmental variation by having greater effects in distal segments [30, 33, 40, 46, 53, 54]. The present results suggest that insulin and ponalrestat, given singly or in combination, can reconstitute some, but not all, of these regional differences.

Vertical differences

Observed increases in height, volume and apex area of epithelial cells in passing from crypt to villous compartments reinforce previous findings but underestimate the differences involved, because they rely on average cell data. In the functional zone of crypts, and on villi, cells show changes in nuclear size, cell size, organelle content and brush border enzyme activity [1, 3, 7, 8, 12, 15, 28, 39, 44, 48–50].

It is interesting to note that there are minor differences in cell width, but major differences in height, as cells pass from crypts to villi. This suggests that cell width is determined before cells exit the crypt compartment and that subsequent changes in volume during migration along the crypt-villus axis are mediated by alterations in cell height. This is consistent with the constraints imposed on lateral variation in cell size by the presence of tight junctions encircling villous epithelial cells. The above applies to differences within a group. However, it appears that between-group differences in the volumes of villous epithelial cells are partly pre-set by intracryptal changes in cell width, on which further changes in cell height are superimposed.

Acknowledgements We wish to thank the Libyan Ministry of Higher Education for supporting Dr. Zoubi's PhD studies in Nottingham and A. Pyper, T. Self and B. Shaw for expert technical assistance.

References

1. Abbas B, Hayes TL, Wilson DJ, Carr KE (1989) Internal structure of the intestinal villus: morphological and morphometric observations at different levels of the mouse villus. *J Anat* 162: 263–273
2. Alison MR, Sarraf CE (1994) The role of growth factors in gastrointestinal cell proliferation. *Cell Biol Int* 18: 1–10
3. Altmann GG (1990) Renewal of the intestinal epithelium: new aspects as indicated by recent ultrastructural observations. *J Electron Microsc Techn* 16: 2–14
4. Altmann GG, Enesco M (1967) Cell number as a measure of distribution and renewal of epithelial cells in the intestine of growing and adult rats. *Am J Anat* 121: 319–336
5. Baddeley AJ, Gundersen HJG, Cruz-Orive L-M (1986) Estimation of surface area from vertical sections. *J Microsc* 142: 259–276
6. Bhoyrul S, Sharma AK, Stribling D, Mirrlees DD, Peterson RG, Farber MO, Thomas PK (1988) Ultrastructural observations on myelinated fibres in experimental diabetes: effect of the aldose reductase inhibitor Ponalrestat given alone or in conjunction with insulin therapy. *J Neurol Sci* 85: 131–147
7. Both NJ de, Dongen JM van, Hofwegen B van, Keulemans J, Visser WJ, Galjaard H (1974) The influence of various cell kinetic conditions on functional differentiation in the small intestine of the rat. A study of enzymes bound to subcellular organelles. *Dev Biol* 38: 119–137
8. Brown AL (1962) Microvilli of the human jejunal epithelial cell. *J Cell Biol* 12: 623–627
9. Buts JP, Keyser N, Romain N, Dandrisosse G, Sokal E, Nsengiyumva T (1994) Response of rat immature enterocytes to insulin: regulation of receptor binding and endoluminal polyamine uptake. *Gastroenterology* 106: 49–59
10. Caspary WF (1973) Effect of insulin and experimental diabetes mellitus on the digestive absorptive function of the small intestine. *Digestion* 9: 248–263
11. Cruz-Orive L-M, Hunzicker EB (1986) Stereology for anisotropic cells: application to growth cartilage. *J Microsc* 143: 47–80
12. Dongen JM van, Visser WJ, Daems WT, Galjaard H (1976) The relation between cell proliferation, differentiation and ultrastructural development in rat intestinal epithelium. *Cell Tissue Res* 174: 183–199
13. Elbrønd VS, Dantzer V, Mayhew TM, Skadhauge E (1991) Avian lower intestine adapts to dietary salt (NaCl) depletion by increasing transepithelial sodium transport and microvillous membrane surface area. *Exp Physiol* 76: 733–744
14. Fogue-Lafitte ME, Marescot MR, Chamblier MC, Rosselin G (1980) Evidence for the presence of insulin binding sites in isolated rat intestinal epithelial cells. *Diabetologia* 19: 373–378
15. Galjaard H, Meer-Flieggen W van der, Both NJ de (1972) Cell differentiation in gut epithelium. In: Viza D, Harris H (eds) *Cell differentiation*. Munksgaard, Copenhagen, pp 322–328
16. Gallo-Payet N, Hugon JS (1984) Insulin receptors in isolated adult mouse intestinal cells: studies in vivo and in organ culture. *Endocrinology* 114: 1885–1892
17. Goodlad RA, Lee CY, Gibbey SG, Ghatei MA, Bloom SR (1993) Insulin and intestinal epithelial cell proliferation. *Exp Physiol* 78: 697–705
18. Gundersen HJG (1979) Estimation of tubule or cylinder L_v , S_v and V_v on thick sections. *J Microsc* 117: 333–345
19. Gundersen HJG, Jensen EB (1985) Stereological estimation of the volume-weighted mean volume of arbitrary particles observed on random sections. *J Microsc* 138: 127–142
20. Gundersen HJG, Jensen EB (1987) The efficiency of systematic sampling and its prediction. *J Microsc* 147: 229–263

21. Heinz-Erian P, Kessler U, Funk B, Gais P, Kiess W (1991) Identification and in situ localisation of the insulin-like growth factor II/mannose-6-phosphate (IGF-II/M6P) receptor in the rat gastrointestinal tract: comparison with the IGF-I receptor. *Endocrinology* 129: 1769–1778
22. Hoffman LA, Yen S, Chang EB (1992) Regional alterations in intestinal sucrase expression in STZ-treated chronically diabetic rats. *Dig Dis Sci* 37: 1078–1083
23. Jervis EL, Levin RJ (1966) Anatomic adaptation of the alimentary tract of the rat to the hyperphagia of chronic alloxan-diabetes. *Nature* 210: 391–393
24. Karasov WH, Diamond JM (1983) Adaptive regulation of sugar and amino acid transport by vertebrate intestine. *Am J Physiol* 245: G443–G462
25. Keelan M, Walker K, Thompson ABR (1985) Intestinal brush border membrane marker enzymes, lipid composition and villus morphology: effect of fasting and diabetes mellitus in rats. *Comp Biochem Physiol [A]* 82: 83–89
26. Laburthe M, Rouyer F, Gammeltoft S (1988) Receptors for insulin-like growth factors I and II in rat gastrointestinal epithelium. *Am J Physiol* 245: G457–G462
27. Lal D, Schedl HP (1974) Intestinal adaptation in diabetes: amino acid absorption. *Am J Physiol* 227: 827–831
28. Leblond CP (1981) The life history of cells in renewing systems. *Am J Anat* 160: 114–158
29. Lorenz-Meyer H, Gottesburen H, Menge H, Bloch R, Riecken EO (1974) Intestinal structure and function in relation to blood sugar levels and food intake in experimental diabetes. In: Dowling RH, Riecken EO (eds) *Intestinal adaptation*. Schattauer, Stuttgart, pp 189–191
30. Mayhew TM (1990) Striated brush border of intestinal absorptive epithelial cells: stereological studies on microvillous morphology in different adaptive states. *J Electron Microscop Technol* 16: 45–55
31. Mayhew TM (1991) The new stereological methods for interpreting functional morphology from slices of cells and organs. *Exp Physiol* 76: 639–665
32. Mayhew TM (1992) A review of recent advances in stereology for quantifying neural structure. *J Neurocytol* 21: 313–328
33. Mayhew TM, Carson FL (1989) Mechanisms of adaptation in rat small intestine: regional differences in quantitative morphology during normal growth and experimental hypertrophy. *J Anat* 164: 189–200
34. Mayhew TM, Middleton C (1985) Crypts, villi and microvilli in the small intestine of the rat. A stereological study of their variability within and between animals. *J Anat* 141: 1–17
35. Mayhew TM, Middleton C, Ross GA (1988) Dealing with oriented surfaces: studies on villi and microvilli of rat small intestine. In: Reith A, Mayhew TM (eds) *Stereology and morphometry in electron microscopy. Problems and solutions*. Hemisphere, New York, pp 85–98
36. Mayhew TM, Carson FL, Sharma AK (1989) Small intestinal morphology in experimental diabetic rats: a stereological study on the effects of an aldose reductase inhibitor (ponalrestat) given with or without conventional insulin therapy. *Diabetologia* 32: 649–654
37. Mayhew TM, Elbrønd VS, Dantzer V, Skadhauge E (1992) Quantitative analysis of factors contributing to expansion of microvillous surface area in the coprodaeum of hens transferred to a low NaCl diet. *J Anat* 181: 73–77
38. Mayhew TM, Elbrønd VS, Dantzer V, Skadhauge E, Møller O (1992) Structural and enzymatic studies on the plasma membrane domains and sodium pump enzymes of absorptive epithelial cells in the avian lower intestine. *Cell Tissue Res* 270: 577–585
39. McElligott TF, Beck IT, Dinda PK, Thompson S (1975) Correlation of structural changes at different levels of the jejunal villus with positive and negative net water transport in vivo and in vitro. *Can J Physiol Pharmacol* 53: 439–450
40. Miller DL, Hanson W, Schedl HP, Osborne JW (1977) Proliferation rate and transit time of mucosal cells in the small intestine of the diabetic rat. *Gastroenterology* 73: 1326–1332
41. Miller S (1975) *Experimental design and statistics*. Methuen, London
42. Nakabou Y, Okita C, Takano Y, Hagiira H (1974) Hyperplastic and hypertrophic changes of the small intestine. *J Nutr Sci Vitaminol (Tokyo)* 20: 227–234
43. Nakabou Y, Ishikawa Y, Misaki A, Hagiira H (1980) Effect of food intake on intestinal absorption and hydrolases in alloxan-diabetic rats. *Metabolism* 29: 181–185
44. Nordstrom C, Dahlqvist A, Josefsson L (1968) Quantitative determination of enzymes in different parts of the villi and crypts of rat small intestine. *J Histochem Cytochem* 15: 713–721
45. Olsen WA, Rosenberg IH (1970) Intestinal transport of sugars and amino acids in diabetic rats. *J Clin Invest* 49: 96–105
46. Olsen W, Agresti HL, Lorentzsonn VW (1974) Intestinal disaccharidases in diabetic rats. In: Dowling RH, Riecken EO (eds) *Intestinal adaptation*. Schattauer, Stuttgart, pp 179–187
47. Park JH, Vanderhoof JA, Blackwood D, MacDonald RG (1990) Characterisation of type I and type II insulin-like growth factor receptors in an intestinal epithelial cell line. *Endocrinology* 126: 2998–3005
48. Pothier P, Hugon JS (1980) Characterization of isolated villus and crypt cells from the small intestine of the adult mouse. *Cell Tissue Res* 211: 405–418
49. Potten CS (1980) Stem cells in small-intestinal crypts. In: Appleton DR, Sunter JP, Watson AJ (eds) *Cell proliferation in the gastrointestinal tract*. Pitman Medical, London, pp 141–154
50. Potten CS, Loeffler M (1987) A comprehensive model of the crypts of the small intestine of the mouse provides insights into the mechanisms of cell migration and the proliferation hierarchy. *J Theor Biol* 127: 381–391
51. Schedl HP, Wilson HD (1971) Effects of diabetes on intestinal growth and hexose transport in the rat. *Am J Physiol* 220: 1739–1745
52. Sokal RR, Rohlf FJ (1981) *Biometry. The principles and practice of statistics in biological research*. Freeman, San Francisco
53. Stenling R, Hagg E, Falkmer S (1984) Stereological studies on the rat small intestinal epithelium. III. Effects of short-term alloxan diabetes. *Virchows Archiv [B]* 47: 263–270
54. Tahara T, Yamamoto T (1988) Morphological changes of the villous microvascular architecture and intestinal growth in rats with streptozotocin-induced diabetes. *Virchows Archiv [A]* 413: 151–158
55. Williams M, Mayhew TM (1992) Responses of enterocyte microvilli in experimental diabetes to insulin and an aldose reductase inhibitor (ponalrestat). *Virchows Archiv [B]* 62: 385–389
56. Wright (1980) Cell proliferation in the normal gastrointestinal tract. Implications for proliferative responses. In: Appleton DR, Sunter JP, Watson AJ (eds) *Cell proliferation in the gastrointestinal tract*. Pitman Medical, London, pp 3–25
57. Young GP, Morton CL, Rose IS, Taranto TM, Bhathal PS (1987) Effects of intestinal adaptation on insulin binding to villus cell membranes. *Gut* 28: 57–62
58. Younoszai MK, Parekh VV, Hoffman JL (1993) Polyamines and intestinal epithelial hyperplasia in streptozotocin-diabetic rats. *Proc Soc Exp Biol Med* 202: 206–211
59. Zoubi SA, Mayhew TM, Sparrow RA (1994) Crypt and villous epithelial cells in adult rat small intestine: numerical and volumetric variation along longitudinal and vertical axes. *Epithelial Cell Biol* 3: 112–118
60. Zoubi SA, Mayhew TM, Sparrow RA (1995) The small intestine in experimental diabetes: cellular adaptation in crypts and villi at different longitudinal sites. *Virchows Arch* 426: 501–507